An electrochemical approach to aluminum-based redox switchable ring opening polymerization

*Zachary C. Hern,[†] Amy Lai, Ramzi N. Massad, Paula L. Diaconescu**

Department of Chemistry and Biochemistry, University of California Los Angeles, Los Angeles, California 90095-1569, United States

ABSTRACT: We report the electrochemically switchable reactivity of (salfen)Al(O^{i}Pr) (salfen = 1,1′-di(2,4-bis-*tert*-butyl-salicylimino)ferrocene) toward the ring opening polymerization of various cyclic esters, ethers, and carbonates. Using a recently developed electrochemical system comprised of an H-cell and a glassy carbon working electrode, an applied potential can alternate between the two redox states of the catalyst and alter monomer incorporation during ring opening polymerization. We discuss differences in activity and control under electrochemical conditions compared to previously studied chemical redox methods and discuss the necessity of a redox switch during certain copolymerization reactions.

INTRODUCTION

New techniques to control polymerization reactions have recently been developed to provide precision over monomer placement. This precise placement of monomers can lead to unique and tunable thermal, mechanical, and degradation properties.[1-10] One way to control such monomer sequence is switchable polymerization,[11-18] where a single, active catalyst can be toggled between

two states that show orthogonal reactivity for various monomers. In particular, for redox switchable reactions,[19-41] sequential redox switches can lead to block copolymers with tunable block compositions and lengths. Recently, electrochemistry has been used to facilitate these redox switches,[42-49] circumventing the need for repeated redox reagent additions and allowing switching through the use of an automated potentiostat. Electrochemical redox switching also offers a precise method of monitoring and measuring the extent of electron transfer while minimizing the number of byproducts. Chemical redox reagents, which typically consist of transition metal compounds, produce byproducts that can be difficult to remove from the final polymer. Additionally, these chemical redox reagents offer little thermodynamic control over the electron transfer process. Conversely, byproducts of an electrochemical event are confined to the counter cell chamber (when an H-cell is used) and thermodynamic control over the electron transfer process is possible via manipulation of the applied potential. Combined, these benefits allow more control over the polymerization reaction, more tailored microstructures, and easier purification when an electrochemical rather than chemical oxidation is employed.

We reported an electrochemical system that is capable of producing tri- and tetrablock copolymers by altering the redox state of a ferrocene-based zirconium complex, (salfan)Zr(O^tBu)$_2$ (salfan = 1,1′-di(2-*tert*-butyl-6-*N*-methylmethylenephenoxy)ferrocene).[45] This system was able to produce ABC triblock and ABAB tetrablock copolymers of L-lactide (LLA), cyclohexene oxide (CHO), and β-butyrolactone (BBL). We hypothesized that this approach would be generally applicable to other redox switchable metal complexes that exhibit unique selectivity toward a large monomer scope. We set out to determine if the electrochemical conditions (i.e., solvent, supporting electrolyte, electrodes) affected other redox switchable polymerization reactions. Herein, we study a previously reported aluminum complex, (salfen)Al(O^iPr) (salfen =

1,1′-di(2,4-bis-*tert*-butyl-salicylimino)ferrocene), and its electrochemically controlled ring-opening polymerization activity. (salfen)Al(O^{i}Pr) bears only one alkoxide initiating group, and we hypothesize that will lead to a greater diffusion constant and more facile electron transfer at the electrode surface compared to the previously studied (salfan)Zr(O^{t}Bu)$_2$.[45] Although the underlying mechanism of ring-opening polymerization of the catalyst remains unchanged,[20,24,28] as evident by the living nature and good control over molecular weight and dispersity, a difference depending on the method of oxidation is apparent, and a comparison of polymers produced from redox-switchable reactions using chemical redox reagents and electrochemical switching is discussed.

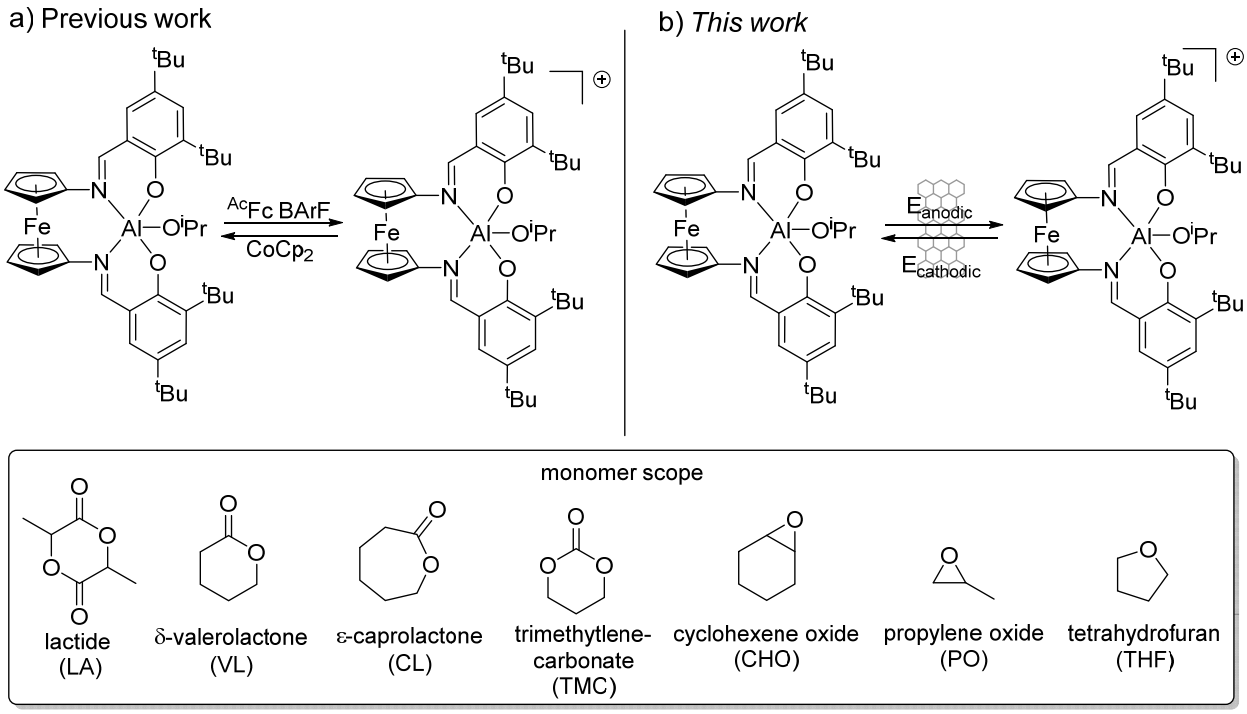

Figure 1. a) Previous work using chemical redox reagents. b) This work using electrochemical switches to produce homo and diblock copolymers. Bottom: Monomer scope of cyclic esters, ethers, and carbonates investigated.

RESULTS AND DISCUSSION

The cyclic voltammogram of (salfen)Al(O^iPr) under bulk electrolysis conditions (75 mM tetrapropylammonium bistriflimide ($TPANTf_2$) in 1,2-difluorobenzene) exhibits a single, reversible electron transfer process with an $E_{1/2}$ = 0.99 V versus Ag/Ag^+ (Figure 2, left, $E_{1/2}$ = 0.24 V versus Fc/Fc^+). When a larger potential window is used (> 1.0 V), an additional electron transfer process is observed (Figure S1); this cyclic voltammogram is largely unchanged compared to using $TPABAr^F$ (BAr^F = tetrakis[3,5-bis(trifluoromethyl)phenyl]borate) as the electrolyte, indicating the change of anion imparts no appreciable difference in the electrochemical electron transfer behavior of (salfen)Al(O^iPr). During bulk electrolysis reactions (Figure 2, right), an oxidative potential of +1.1 V (versus Ag/Ag^+) was applied to avoid secondary oxidations. The current versus time plot exhibits a fairly steady current of ca. 0.35 mA until about 0.8 Coulombs of charge is passed. Then, the current decreases and charge transfer (Q) plateaus near 0.96 C, the theoretical charge transfer of 0.01 mmol electrons. In total, the complete oxidation of (salfen)Al(O^iPr) takes 45 minutes, about 15 minutes less than in the case of (salfan)Zr($O^tBu)_2$.[45] This may suggest the smaller aluminum complex diffuses more readily to the electrode surface than (salfan)Zr($O^tBu)_2$, which has an additional alkoxide group coordinated to the metal ion.

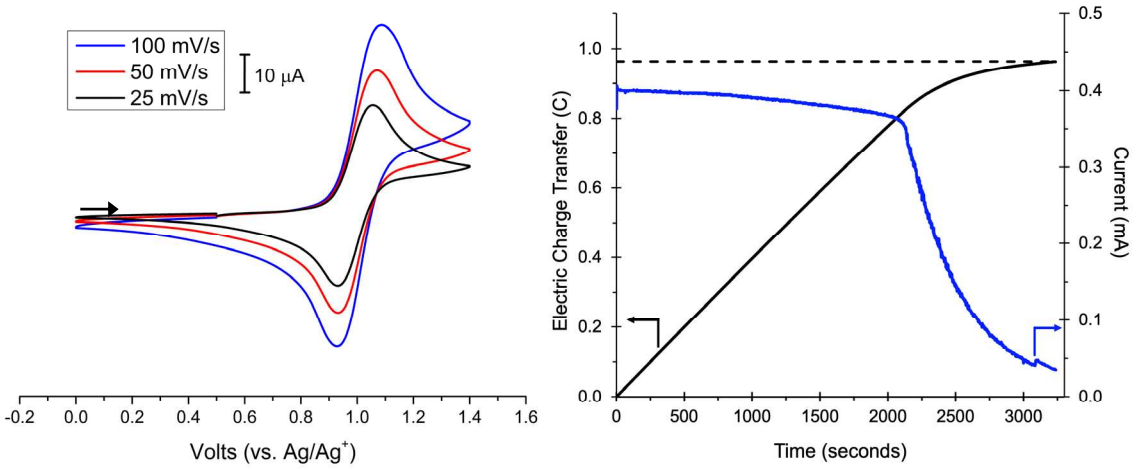

Figure 2. Cyclic voltammogram of 2.5 mM (salfen)Al(O^{i}Pr) in 100 mM TPANTf$_2$ in 1,2-difluorobenzene (left). Representative bulk electrolysis trace of 0.01 mmol (salfen)Al(O^{i}Pr) under electrolysis conditions used for polymerization (right). The dotted line represents the theoretical charge transfer of 0.01 mmol electrons.

We set out to investigate if our electrochemical reaction conditions had an effect on homopolymerization reactions catalyzed by (salfen)Al(O^{i}Pr). We previously reported that in C_6D_6, LA and TMC polymerization proceeded with (salfen)Al(O^{i}Pr) in the reduced state but not the oxidized state, while CHO exhibits the opposite reactivity. δ-Valerolactone (VL) and ε-caprolactone (CL) showed activity in both oxidation states.

First, homopolymerization reactions of LA and TMC were carried out with (salfen)Al(O^{i}Pr) in the reduced state in the presence of TPANTf$_2$ in 1,2-difluorobenzene. We found that both reactions became slower under these electrochemically relevant conditions. Specifically, LA polymerization proceeded at 100 ºC, reaching a conversion of 37% in 24 hours (compared to 64% in 24 hours when using previously reported conditions, Figure S2). A similar reaction, using 1,2-difluorobenzene as the solvent and excluding the electrolyte, showed 40% conversion in 24 hours

at 100 ºC (Figure S3), suggesting the presence of electrolyte did not have an effect on the reaction rate and, instead, the solvent choice was responsible for activity differences. Similarly, TMC homopolymerization proceeded more sluggishly at room temperature (Figure S4), reaching 74% conversion in 3.5 hours (compared to 98% in only 2.5 hours). Both VL and CL showed similar trends of slower reactions rates (Table 1, entries 5 and 7, Figures S7 & S9, respectively). Expectedly, no cyclic ethers (CHO, PO, THF) were polymerized by (salfen)Al(O^iPr) in the reduced state (Table 1, entry 9). In all reduced state scenarios, the experimental and theoretical molecular weights showed better agreement under electrochemical than previously reported chemical redox conditions, likely due to slower reactions in 1,2-difluorobenzene than in C_6D_6, leading to a better controlled polymerization.

We next moved to the polymerization activity of the electrochemically generated oxidized form of (salfen)Al(O^iPr). The first major difference was the rapid polymerization of TMC, which reached nearly a full conversion in under 15 minutes (compared to no activity for the chemically generated counterpart).[28] The rapid conversion, however, did not lead to a complete lack of control, as evident by the molecular weight (11.8 kDa) showing a moderate agreement to the experimental value (9.6 kDa) and a dispersity of 1.5. However, both oxidation states produced polymers with a bimodal trace at high conversions as determined by size exclusion chromatography (SEC). When TMC loading was increased to 200 equivalents, the polymer produced by the reduced complex at moderate conversion (< 60%) resulted in a unimodal trace with a narrow dispersity. As conversion increased (> 80%), the trace became bimodal (Figure S24), suggesting a loss of control at higher conversion—a phenomenon that was reported previously.[50] Since activity toward TMC in the oxidized state is unusual, we decided to find out whether it is due to the change in solvent, and/or the presence of $TPANTf_2$. When the results of using a chemical oxidant in 1,2-difluorobenzene

were similar to those obtained with the electrochemically generated species, a new batch of (salfen)Al(O^iPr) and carefully purified $^{Ac}FcBAr^F$ were employed (see Experimental section for details). These experiments showed that indeed, [(salfen)Al(O^iPr)][BAr^F] has similar activity toward TMC as the electrochemically generated species (Figure S6). LA showed no conversion in the oxidized state, while both CL and VL did, both faster than in the reduced state.

Notably, the electrochemically generated oxidized catalyst showed a much better agreement between the theoretical and experimental molecular weight with a lower dispersity for VL polymerization compared to the chemical counterpart (Table 1, entry 6). However, the opposite trend was true for CL, where chemical oxidation showed a better molecular weight agreement with a more narrow dispersity than electrochemical oxidation. The disparity, however, was far less drastic in the VL electrochemical (2x greater) versus chemical oxidation (5x greater), suggesting the electrochemical oxidation generally leads to a more controlled polymerization process overall. Additionally, CL polymerization proceeded at similar rates in both the reduced and oxidized state regardless of the oxidation method (chemical or electrochemical), indicating CL polymerization is less prone to changes in the oxidation state of the catalyst, as previously reported.[51] Lastly, cyclic ethers were surveyed and showed a drastic difference compared to when using chemical redox reagents. Specifically, the homopolymerization of CHO with the oxidized catalyst generated electrochemically reached 75% conversion in 21 hours (Table 1, entry 10, Figure S11), in comparison to 99% in only 0.1 hours for the chemically controlled reaction.[28] Other cyclic ethers (PO and THF) showed no activity (Table 1, entries 11 & 12).

End group analysis was performed on homopolymers produced from the electrochemically oxidized catalyst to ensure cationic polymerization did not occur from electrochemical byproducts and only a coordination-insertion mechanism operated, as previously shown for similar ferrocene-

based redox-switchable complexes.[24,40,52,53] ^{1}H NMR spectra of PVL (Table 1 entry, 6) and PCL (Table 1, entry 8) contain a doublet peak at ca. 1.20 ppm, corresponding to the methyl groups of the isopropoxide initiator (Figures S28 and S29). The ratio of the isopropoxide protons to the bulk polymer protons give calculated polymer molecular weights of 14.7 kDa and 21.5 kDa for PVL and PCL, respectively. These molecular weights show good agreement with the experimental molecular weights determined by size-exclusion chromatography (14.5 kDa and 20.2 kDa, respectively), suggesting the majority of polymers isolated was generated from the aluminum isopropoxide species and not a cationic or anionic species produced during electrolysis. Alkoxide end groups for PCHO and PTMC could not be identified due to overlapping polymer proton peaks.

Table 1. Electrochemical homopolymerization reactions of various monomers.

entry	**mon.**	**cat.**	**conv.[a] (time, h)**	**$M_{n,\ theor.}$ (kDa)**	**$M_{n,\ exp.}$ (kDa)[b]**	**Đ**	**conv. (time, h)**	**$M_{n,\ theor.}$ (kDa)**	**$M_{n,\ exp.}$ (kDa) (Đ)**
			Electrochemical Oxidation (this work)				**Chemical Oxidation[28]**		
1	LA	red	37% (24)	5.3	4.5	1.1	64% (24)	9.2	7.5 (1.0)
2	LA	ox	NR (24)	--	--	--	NR	--	--
3	TMC	red	74% (3.5)	7.4	7.2	1.3	98% (2.5)	10.0	19.6 (1.0)
4	TMC	ox	94% (0.2)	9.6	11.8	1.5	0% (23)	--	--
5	VL	red	72% (5.5)	7.2	14.1	1.1	90% (2)	9.0	35.4 (1.0)
6	VL	ox	98% (0.2)	9.8	14.5	1.1	87% (1.2)	8.7	42.1 (1.4)

7	CL	red	87% (5)	9.9	11.7	1.1	92% (2)	10.5	19.3 (1.0)
8	CL	ox	77% (4)	8.8	20.2	1.4	92% (1)	10.5	16.1 (1.1)
9[#]	CHO	red	NR (24)	--	--	--	NR	--	--
10[#]	CHO	ox	75% (21)	14.5	12.4	1.3	99% (0.1)	19.6	20.9 (1.5)

Conditions: 75 mM solution $TPANTf_2$, 1.5 mL 1,2-difluorobenzene. 0.01 mmol precatalyst, 100 equivalents monomer, unless otherwise noted; all polymerizations were carried out at room temperature except for LA, which was carried out at 100 ºC; red = (salfen)Al(O^iPr); ox = [(salfen)Al(OiPr)][NTf_2]; [a] determined by ^1H NMR spectroscopy by integrating polymer to monomer peaks; [b] determined by SEC. [#] 200 equivalents used.

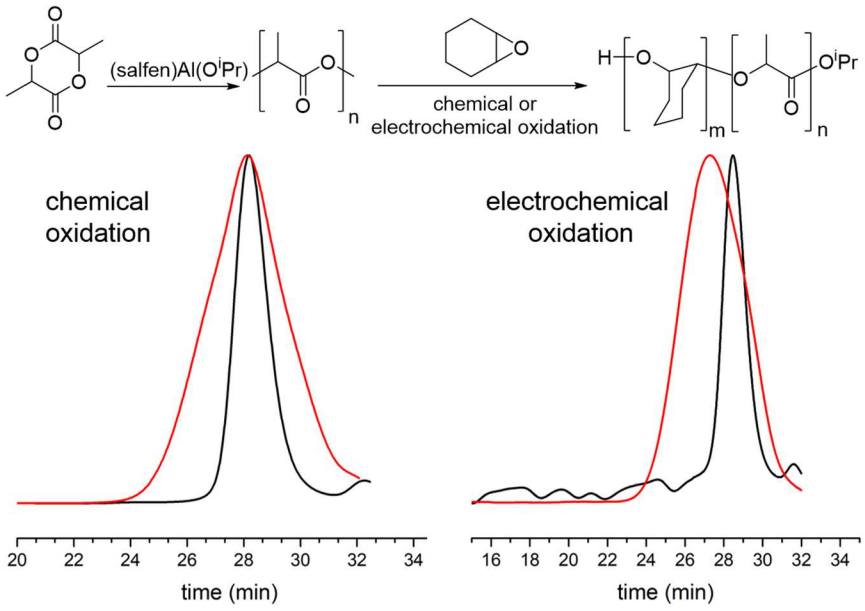

Figure 3. Comparison of PHCO-b-PLA block copolymers produced by (salfen)Al(O^iPr) via a chemical redox switch (left) and an electrochemical switch (right).

Next, we moved to copolymerization reactions where the increased control of the electrochemically oxidized aluminum complex was more evident. Two PCHO-b-PLA copolymers were synthesized, one using an electrochemical switch and the other a chemical switch. For a direct

comparison, the chemical redox switch was performed using electrochemical conditions (e.g., 75 mM solution of $TPANTf_2$ in 1,2-difluorobenzene), but with a chemical oxidant ($^{Ac}FcNTf_2$, ^{Ac}Fc = acetylferrocenium) in place of electrochemistry. The initial LA polymerization by the reduced complex proceeded as usual, however, the incorporation of CHO in the second block proceeded more quickly, reaching 72% conversion in 2.5 h (compared to 67% in 16 h). The diblock copolymer produced chemically exhibited a broad SEC trace with a dispersity of 1.7 (Table 2, entry 1). Additionally, the peak of the SEC trace remained at the same retention time, and only broadened (both to greater and smaller retentions times), indicating the process was less controlled and only a minority of polymer chain ends incorporated CHO. On the other hand, when the oxidation was performed electrochemically, CHO incorporation occurred more slowly and the final copolymer exhibited a lower molecular weight with a narrower dispersity of 1.2 (Table 2, entry 2) than observed for the chemical oxidation. Additionally, the peak of the SEC trace decreased in retention time indicating the majority of the polymer chains increased in molecular weight. Furthermore, both PLA and PCHO showed the same diffusion coefficients by diffusion ordered spectroscopy (DOSY), confirming the formation of a copolymer (Figures S25 & S26).

Table 2. Electrochemical copolymerization reactions with (salfen)Al(O^iPr).

entry	**mon. 1 (conv.)[a]**	**mon. 2 (conv.)[a]**	**cat. (time, h)**	**$M_{n,\,theor.}$ (kDa)[b]**	**$M_{n,\,exp.}$ (kDa)[b]**	**Đ**
1[c]	LA (41%)	CHO (72%)	red-ox (24-2.5)	5.9 (20.0)	6.2 (19.7)	1.0 (1.7)
2	LA (37%)	CHO (67%)	red-ox (22-16)	5.3 (18.5)	5.8 (13.5)	1.1 (1.2)

3	TMC (56%)	CHO (77%)	red-ox (2.5-18)	5.7 (20.8)	6.0 (26.1)	1.3 (1.4)
4	TMC (97%)	CHO (46%)	ox-ox (0.2-3)	9.9 (18.9)	10.8 (11.6)	1.5 (3.0)
5	LA (59%)	TMC (5%)	red-ox (24-24)	--	N.D.	N.D.
6	LA (59%)	TMC (9%)	red-red (2-24)	--	N.D.	N.D.

Conditions: 75 mM solution $TPANTf_2$, 1.5 mL 1,2-difluorobenzene. 0.01 mmol precatalyst, 100 equiv monomer 1 and 200 equiv monomer 2; red = (salfen)Al(O^iPr); ox = [(salfen)Al(O^iPr)][NTf_2]; [a] determined by ^1H NMR spectroscopy by integrating polymer to monomer peaks and reported as conversion of that monomer; [b] determined by SEC; [c] using the chemical method. Molecular weights and dispersities are reported for the first block only and the final copolymer in parentheses.

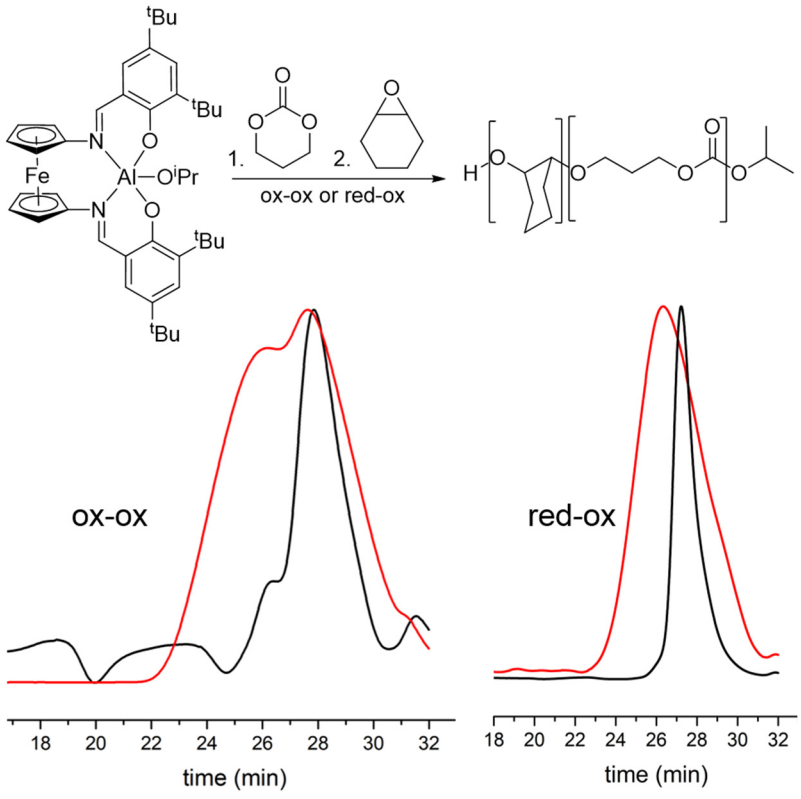

Figure 4. SEC traces of a TMC and CHO copolymerization reaction using an ox-ox redox switch (left) and a red-ox redox switch (right). Black trace represents the first polymerization step and the red trace represents the second step.

Since the polymerization of TMC proceeded with (salfen)Al(O^iPr) in both the reduced and oxidized state, we set out to determine if the oxidation state had an effect on copolymers containing a TMC block. First, PCHO-b-PTMC copolymers were synthesized using both an oxidized-oxidized catalyst state and a reduced-oxidized catalyst state (Figures S14 & S15) employing the electrochemical setup. The reduced-oxidized catalyst system proceeded with 56% and 77% TMC and CHO conversion, respectively, and yielded a diblock copolymer with a unimodal SEC trace, a molecular weight of 26.1 kDa and a dispersity of 1.4 (Figure 4), and a single diffusion coefficient in DOSY (Figure S27). On the other hand, because TMC polymerization in the oxidized state proceeds rapidly and uncontrolled, the diblock polymer had a bimodal SEC trace (similar to that of the PTMC trace) with a dispersity of 3.0, suggesting either both PTMC polymeric species chain extended during the second polymerization step or a mixture of homopolymers was produced. The molecular weight of the initial TMC polymerization step (10.8 kDa) and that of the final polymer produced after CHO polymerization (11.6 kDa) were similar and deviated from the theoretical molecular weight if a diblock copolymer were formed (18.9 kDa), suggesting the bimodal SEC peaks correspond to the two homopolymers, PTMC and PCHO. Additionally, the dispersity of 3.0 suggests the presence of two homopolymer species. Unfortunately, chain end analysis of the polymer sample could not differentiate between the two homopolymers due to their molecular weights and the number of broad polymer peaks in the 1-3 ppm range, masking any peaks corresponding to an alkoxide end-group. However, the junction between the PTMC block and

PCHO block in a diblock copolymer is evident by the peak around 3.15 ppm (red-ox catalyst switch, Figure S14) which is notably absent in the polymer ^{1}H NMR when using an ox-ox switch (Figure S15). Combined, these two copolymerization reactions highlight the necessity of a redox switch when attempting to produce a PCHO-b-PTMC copolymer using a catalyst system.

Attempts to synthesize PTMC-b-PLA block copolymers, both by a reduced-reduced and a reduced-oxidized (generated electrochemically) catalyst state afforded mostly PLA homopolymers with less than 10% TMC conversion. ^{1}H NMR spectra of the isolated polymers also indicated little TMC incorporation. This result was expected as TMC incorporation after LA polymerization is rare in the literature.

CONCLUSIONS

In conclusion, (salfen)Al(O^{i}Pr) exhibits similar reactivity when using an electrochemical switch compared to a chemical redox switch, with the notable exception of trimethylene carbonate. In the reduced state, lactide, lactones, and TMC are polymerized with good control, while cyclic ethers show no activity. In the electrochemically generated oxidized state, CHO is polymerized relatively slowly and with better control than when using a chemical oxidant. However, other cyclic ethers such as THF and PO showed no activity. Both lactide and cyclohexene oxide were the only two monomers that exhibit orthogonal reactivity (LA in the reduced state and CHO in the oxidized state) and both lactones (VL and CL) and TMC are ring opened in both oxidation states. The necessity of a redox switch is shown when producing well controlled diblock copolymers, namely PCHO-b-PLA and PCHO-b-PTMC.

EXPERIMENTAL SECTION

General considerations and procedures. All air-sensitive experiments were performed under a dry nitrogen atmosphere in an MBraun inert-gas glovebox. Unless otherwise noted, solvents were purified using a two-column solid-state purification system by the method of Grubbs[54] and transferred to the glovebox without exposure to air. (salfen)Al(O^iPr)[28] and $TPANTf_2$[45] were synthesized according to literature procedures. $^{Ac}FcBAr^F$ [55] and $^{Ac}FcNTf$[28] were synthesized and purified according to literature procedures and crystallized three times before use. The purity of the paramagnetic oxidants was determined by elemental analysis. NMR solvents were obtained from Cambridge Isotope Laboratories, degassed, and stored over activated molecular sieves prior to use. L-Lactide was purchased from VWR, crystallized from ethyl acetate, and dried before use. Cyclohexene oxide, propylene oxide, and styrene oxide was purchased from Fischer Scientific and dried over CaH_2, distilled under reduced pressure, and then brought into the glovebox without exposure to air. 1,2-difluorobenzene was dried over CaH_2, distilled under nitrogen, and degassed using three cycles of freeze-pump-thaw. Lithium bis(trifluoromethanesulfonyl)imide ($LiNTf_2$) and tetra-*n*-propylammonium chloride (TPACl) were purchased from Fisher Scientific and used as received. Magnesium foil was purchased from Sigma Aldrich and used as received.

NMR spectra were recorded on Bruker AV300, Bruker AV-400, Bruker AV-500, and DRX-500 spectrometers at room temperature. ^1H NMR and ^{13}C NMR spectra and chemical shifts are reported with respect to an internal solvent: 7.16 ppm (C_6D_6) and 7.26 ($CDCl_3$). Polymer molecular weights were determined by SEC using an SEC-MALS instrument, equipped with Shimazu Prominence-I LC 2030 C 3D autosampler, two MZ Analysentechnik MZ-Gel SDplus LS 5 μm, 300 × 8 mm linear columns, Wyatt DAWN HELOS-II, and a Wyatt Optilab T-rEX. The column temperature was set to 40°C, flow rate to 0.700 mL/min, and all samples were dissolved

in HPLC grade THF. The dn/dc values, molar mass, dispersity values were calculated from the RI signal by using the 100% mass recovery method in the Astra software and a known sample concentration.

General polymerization procedures. Polymerization reactions were performed in 1.6 mL of a 75 mM $TPANTf_2$ solution in 1,2-difluorobenzene. All L-lactide polymerizations were performed outside the glovebox in a Schlenk tube at 100 ºC with stirring. Cyclic ether and trimethylene carbonate (TMC) polymerizations were carried out in a 20 mL scintillation vial at room temperature inside the glovebox with stirring. Unless otherwise noted, 0.01 mmol of (salfen)Al(O^iPr) and 100 equivalents of monomer were used. For reactions requiring electrolysis before polymerization, the electrolysis reaction was completed before adding appropriate monomer. For sequential addition polymerization reactions, the monomer was added after the electrolysis event needed to convert the catalyst into its active state for that monomer. For one-pot polymerization reactions, all monomers were added at the beginning and subjected to the mentioned reaction/bulk electrolysis conditions, unless otherwise noted. For copolymer reactions, 0.1 mL aliquots were taken and combined with 0.3 mL C_6D_6 for ^1H NMR analysis. The sample was then precipitated in methanol, centrifuged for 15 minutes, decanted, and dried under vacuum for SEC analysis.

General electrochemistry considerations. All electrochemistry experiments (including bulk electrolysis) were conducted at room temperature using a CH Instruments 630D potentiostat and recorded with CH Instruments software version (13.04) with data processing on Origin 9.1. All potentials are referenced to Ag/Ag^+. Custom H-cells were fitted with an ultrafine frit from Ace glassware (10 mm x 3 mm, 0.9-1.4 μm porosity) and blown at the Caltech glassblowing facilities. Each half chamber has a volume of ca. 1.6 mL. For cyclic voltammetry experiments, one chamber

was designated as the working chamber with 5 mM (salfen)Al(O^iPr) in a 75 mM solution of $TPANTf_2$ in 1,2-difluorobenzene. A glassy carbon working electrode (planar circular area = 0.071 cm^2) and separated silver wire pseudoreference electrode were affixed. The counter chamber contained a magnesium foil counter electrode (10 mm x 100 mm). Experiments were conducted with an automatic 90% iR compensation using CHInstruments software. For bulk electrolysis reactions, one chamber was designated the working chamber and affixed with a carbon plate working electrode (25 mm x 7 mm) and a Teflon-tip separated Ag/Ag^+ pseudoreference electrode (CH Instruments), and two stir bars (10 mm and 5 mm). The second chamber was designated the counter chamber and affixed with a magnesium foil counter electrode (10 mm x 100 mm, Sigma Aldrich). Silver wire and magnesium foil electrodes were placed in the glovebox antechamber and placed under vacuum overnight before bringing into the glovebox. The glassy carbon plate was polished sequentially with 1.0 μm, 0.3 μm, and 0.05 μm alumina in water on a polishing pad, sonicated in acetone for 5 minutes, and placed in an oven overnight before bringing into the glovebox. Each chamber contained ca 1.6 mL of a 75 mM solution of tetra-*n*-propylammonium bis(trifluoromethanesulfonyl)imide ($TPANTf_2$) in 1,2-difluorobenzene. Anodic electrolysis was performed at +0.8 V versus Ag/Ag^+ and cathodic electrolysis was performed at -0.1 V versus Ag/Ag^+.[28]

Supporting Information. The following files are available free of charge. Characterization data (PDF)

AUTHOR INFORMATION

Corresponding Author

Paula L. Diaconescu – Department of Chemistry and Biochemistry, University of California Los Angeles, Los Angeles, California 90095-1569 United States; email: pld@chem.ucla.edu

Present Address

† HRL Laboratories, Malibu, CA

Author Contributions

The manuscript was written through contributions of all authors. All authors have given approval to the final version of the manuscript.

Notes

The authors declare no competing financial interest.

ACKNOWLEDGMENTS

This work was supported by the NSF (Grant CHE-1809116 and CHE-2400314 to PLD, and CHE-1048804 for NMR spectroscopy) and UCLA. ZCH and RNM were supported in part by an NRT-INFEWS Grant (No. DGE-1735325).

REFERENCES

(1) Li, J.; Stayshich, R. M.; Meyer, T. Y. Exploiting Sequence To Control the Hydrolysis Behavior of Biodegradable PLGA Copolymers. *J. Am. Chem. Soc.* **2011,** *133* (18), 6910.
(2) Peng, C.; Joy, A. Alternating and random-sequence polyesters with distinct physical properties. *Polym. Chem.* **2017,** *8* (15), 2397.
(3) Yokota, K.; Kougo, T.; Hirabayashi, T. Syntheses and Properties of Periodic Copolymers. *Polym. J.* **1983,** *15* (5), 349.
(4) Deacy, A. C.; Gregory, G. L.; Sulley, G. S.; Chen, T. T. D.; Williams, C. K. Sequence Control from Mixtures: Switchable Polymerization Catalysis and Future Materials Applications. *J. Am. Chem. Soc.* **2021**, DOI:10.1021/jacs.1c03250 10.1021/jacs.1c03250.
(5) Hosseini, K.; Goonesinghe, C.; Roshandel, H.; Chang, J.; Nyamayaro, K.; Jung, H.-J.; Diaconescu, P. L.; Mehrkhodavandi, P. Mechanistic Insights into Selective Indium-Catalyzed Coupling of Epoxides and Lactones. *ACS Catal.* **2023**, DOI:10.1021/acscatal.3c03450 10.1021/acscatal.3c03450, 13195.

(6) Nowalk, J. A.; Swisher, J. H.; Meyer, T. Y. Influence of Short-Range Scrambling of Monomer Order on the Hydrolysis Behaviors of Sequenced Degradable Polyesters. *Macromolecules* **2019,** *52* (12), 4694.
(7) Lu, Y.; Swisher, J. H.; Meyer, T. Y.; Coates, G. W. Chirality-Directed Regioselectivity: An Approach for the Synthesis of Alternating Poly(Lactic-co-Glycolic Acid). *J. Am. Chem. Soc.* **2021,** *143* (11), 4119.
(8) Zhang, Z.; Shi, C.; Scoti, M.; Tang, X.; Chen, E. Y. X. Alternating Isotactic Polyhydroxyalkanoates via Site- and Stereoselective Polymerization of Unsymmetrical Diolides. *J. Am. Chem. Soc.* **2022,** *144* (43), 20016.
(9) Diaz, C.; Mehrkhodavandi, P. Strategies for the synthesis of block copolymers with biodegradable polyester segments. *Polym. Chem.* **2021,** *12* (6), 783.
(10) Aluthge, D. C.; Xu, C.; Othman, N.; Noroozi, N.; Hatzikiriakos, S. G.; Mehrkhodavandi, P. PLA–PHB–PLA Triblock Copolymers: Synthesis by Sequential Addition and Investigation of Mechanical and Rheological Properties. *Macromolecules* **2013,** *46* (10), 3965.
(11) Deng, S.; Jolly, B. J.; Wilkes, J. R.; Mu, Y.; Byers, J. A.; Do, L. H.; Miller, A. J. M.; Wang, D.; Liu, C.; Diaconescu, P. L. Spatiotemporal control for integrated catalysis. *Nat. Rev. Methods Primers* **2023,** *3*, 28.
(12) Chen, G.; Xia, L.; Wang, F.; Zhang, Z.; You, Y.-Z. Recent progress in the construction of polymers with advanced chain structures via hybrid, switchable, and cascade chain-growth polymerizations. *Polym. Chem.* **2021,** *12* (26), 3740.
(13) Zhao, Y.; Wang, Y.; Zhou, X.; Xue, Z.; Wang, X.; Xie, X.; Poli, R. Oxygen-Triggered Switchable Polymerization for the One-Pot Synthesis of CO2-Based Block Copolymers from Monomer Mixtures. *Angew. Chem. Int. Ed.* **2019,** *58* (40), 14311.
(14) Stößer, T.; Sulley, G. S.; Gregory, G. L.; Williams, C. K. Easy access to oxygenated block polymers via switchable catalysis. *Nat. Commun.* **2019,** *10* (1), 2668.
(15) Ihrig, S. P.; Eisenreich, F.; Hecht, S. Photoswitchable polymerization catalysis: state of the art, challenges, and perspectives. *Chem. Commun.* **2019,** *55* (30), 4290.
(16) Peris, E. Smart N-Heterocyclic Carbene Ligands in Catalysis. *Chem. Rev.* **2018,** *118* (19), 9988.
(17) Eisenreich, F.; Kathan, M.; Dallmann, A.; Ihrig, S. P.; Schwaar, T.; Schmidt, B. M.; Hecht, S. A photoswitchable catalyst system for remote-controlled (co)polymerization in situ. *Nat. Catal.* **2018,** *1* (7), 516.
(18) Hu, C.; Pang, X.; Chen, X. Self-Switchable Polymerization: A Smart Approach to Sequence-Controlled Degradable Copolymers. *Macromolecules* **2022,** *55* (6), 1879.
(19) Lai, A.; Hern, Z. C.; Shen, Y.; Dai, R.; Diaconescu, P. L. In *Comprehensive Coordination Chemistry III*; Constable, E. C.;Parkin, G.;Que Jr, L., Eds.; Elsevier: Oxford, 2021, DOI:https://doi.org/10.1016/B978-0-08-102688-5.00044-1 https://doi.org/10.1016/B978-0-08-102688-5.00044-1.
(20) Wei, J.; Diaconescu, P. L. Redox-switchable Ring-opening Polymerization with Ferrocene Derivatives. *Acc. Chem. Res.* **2019,** *52* (2), 415.
(21) Huang, W.; Diaconescu, P. L. Reactivity and Properties of Metal Complexes Enabled by Flexible and Redox-Active Ligands with a Ferrocene Backbone. *Inorg. Chem.* **2016,** *55* (20), 10013.

(22) Biernesser, A. B.; Delle Chiaie, K. R.; Curley, J. B.; Byers, J. A. Block Copolymerization of Lactide and an Epoxide Facilitated by a Redox Switchable Iron-Based Catalyst. *Angew. Chem. Int. Ed.* **2016,** *55* (17), 5251.
(23) Biernesser, A. B.; Li, B.; Byers, J. A. Redox-Controlled Polymerization of Lactide Catalyzed by Bis(imino)pyridine Iron Bis(alkoxide) Complexes. *J. Am. Chem. Soc.* **2013,** *135* (44), 16553.
(24) Quan, S. M.; Wei, J.; Diaconescu, P. L. Mechanistic Studies of Redox-Switchable Copolymerization of Lactide and Cyclohexene Oxide by a Zirconium Complex. *Organometallics* **2017,** *36* (22), 4451.
(25) Abubekerov, M.; Vlček, V.; Wei, J.; Miehlich, M. E.; Quan, S. M.; Meyer, K.; Neuhauser, D.; Diaconescu, P. L. Exploring Oxidation State-Dependent Selectivity in Polymerization of Cyclic Esters and Carbonates with Zinc(II) Complexes. *iScience* **2018,** *7*, 120.
(26) Abubekerov, M.; Khan, S. I.; Diaconescu, P. L. Ferrocene-bis(phosphinimine) Nickel(II) and Palladium(II) Alkyl Complexes: Influence of the Fe–M (M = Ni and Pd) Interaction on Redox Activity and Olefin Coordination. *Organometallics* **2017,** *36* (22), 4394.
(27) Abubekerov, M.; Shepard, S. M.; Diaconescu, P. L. Switchable Polymerization of Norbornene Derivatives by a Ferrocene-Palladium(II) Heteroscorpionate Complex. *Eur. J. Inorg. Chem.* **2016,** *2016* (15-16), 2634.
(28) Lai, A.; Hern, Z. C.; Diaconescu, P. L. Switchable Ring-Opening Polymerization by a Ferrocene Supported Aluminum Complex. *ChemCatChem* **2019,** *11* (16), 4210.
(29) Lowe, M. Y.; Shu, S.; Quan, S. M.; Diaconescu, P. L. Investigation of redox switchable titanium and zirconium catalysts for the ring opening polymerization of cyclic esters and epoxides. *Inorg. Chem. Front.* **2017,** *4*, 1798.
(30) Shawver, N. M.; Doerr, A. M.; Long, B. K. A perspective on redox-switchable ring-opening polymerization. *J. Polym. Sci.* **2023,** *61* (5), 361.
(31) Doerr, A. M.; Burroughs, J. M.; Legaux, N. M.; Long, B. K. Redox-switchable ring-opening polymerization by tridentate ONN-type titanium and zirconium catalysts. *Catal. Sci. Technol.* **2020,** *10* (19), 6501.
(32) Doerr, A. M.; Burroughs, J. M.; Gitter, S. R.; Yang, X.; Boydston, A. J.; Long, B. K. Advances in Polymerizations Modulated by External Stimuli. *ACS Catal.* **2020,** *10* (24), 14457.
(33) Kaiser, J. M.; Long, B. K. Recent developments in redox-active olefin polymerization catalysts. *Coord. Chem. Rev.* **2018,** *372*, 141.
(34) Ahumada, G.; Ryu, Y.; Bielawski, C. W. Potentiostatically Controlled Olefin Metathesis. *Organometallics* **2020,** *39* (10), 1744.
(35) Lastovickova, D. N.; Teator, A. J.; Shao, H.; Liu, P.; Bielawski, C. W. A redox-switchable ring-closing metathesis catalyst. *Inorg. Chem. Front.* **2017,** *4* (9), 1525.
(36) Lastovickova, D. N.; Shao, H.; Lu, G.; Liu, P.; Bielawski, C. W. A Ring-Opening Metathesis Polymerization Catalyst That Exhibits Redox-Switchable Monomer Selectivities. *Chem. Eur. J.* **2017,** *23* (25), 5994.
(37) Teator, A. J.; Lastovickova, D. N.; Bielawski, C. W. Switchable Polymerization Catalysts. *Chem. Rev.* **2016,** *116* (4), 1969.
(38) Varnado, C. D.; Jr; Rosen, E. L.; Collins, M. S.; Lynch, V. M.; Bielawski, C. W. Synthesis and study of olefin metathesis catalysts supported by redox-switchable diaminocarbene[3]ferrocenophanes. *Dalton Trans.* **2013,** *42* (36), 13251.

(39) Arumugam, K.; Varnado, C. D.; Sproules, S.; Lynch, V. M.; Bielawski, C. W. Redox-Switchable Ring-Closing Metathesis: Catalyst Design, Synthesis, and Study. *Chem. Eur. J.* **2013,** *19* (33), 10866.
(40) Wei, J.; Riffel, M. N.; Diaconescu, P. L. Redox Control of Aluminum Ring-Opening Polymerization: A Combined Experimental and DFT Investigation. *Macromolecules* **2017,** *50* (5), 1847.
(41) Li, S.; Davis, A. R.; Roshandel, H.; Adhami, N.; Shen, Y.; Co, N. H.; Morag, L. A.; Etemad, H.; Liu, Y.; Diaconescu, P. L. Application of a ferrocene-chelating heteroscorpionate ligand in nickel mediated radical polymerization. *Inorg. Chem. Front.* **2024,** *11* (12), 3511.
(42) Qi, M.; Zhang, H.; Dong, Q.; Li, J.; Musgrave, R. A.; Zhao, Y.; Dulock, N.; Wang, D.; Byers, J. A. Electrochemically switchable polymerization from surface-anchored molecular catalysts. *Chem. Sci.* **2021,** *12*, 9042.
(43) Qi, M.; Dong, Q.; Wang, D.; Byers, J. A. Electrochemically Switchable Ring-Opening Polymerization of Lactide and Cyclohexene Oxide. *J. Am. Chem. Soc.* **2018,** *140* (17), 5686.
(44) Peterson, B. M.; Lin, S.; Fors, B. P. Electrochemically Controlled Cationic Polymerization of Vinyl Ethers. *J. Am. Chem. Soc.* **2018,** *140* (6), 2076.
(45) Hern, Z. C.; Quan, S. M.; Dai, R.; Lai, A.; Wang, Y.; Liu, C.; Diaconescu, P. L. ABC and ABAB Block Copolymers by Electrochemically Controlled Ring-Opening Polymerization. *J. Am. Chem. Soc.* **2021,** *143* (47), 19802.
(46) Shen, Y.; Mu, Y.; Wang, D.; Liu, C.; Diaconescu, P. L. Tuning Electrode Reactivity through Organometallic Complexes. *ACS Appl. Mater. Interfaces* **2023,** *15* (24), 28851.
(47) Wang, X.; Chin, A. L.; Zhou, J.; Wang, H.; Tong, R. Resilient Poly(α-hydroxy acids) with Improved Strength and Ductility via Scalable Stereosequence-Controlled Polymerization. *J. Am. Chem. Soc.* **2021,** *143* (40), 16813.
(48) Wang, X.; Huo, Z.; Xie, X.; Shanaiah, N.; Tong, R. Recent Advances in Sequence-Controlled Ring-Opening Copolymerizations of Monomer Mixtures. *Chem. Asian J.* **2023,** *18* (4), e202201147.
(49) Dai, R.; Diaconescu, P. L. Investigation of a Zirconium Compound for Redox Switchable Ring Opening Polymerization. *Dalton Trans.* **2019,** *48*, 2996.
(50) Delcroix, D.; Martín-Vaca, B.; Bourissou, D.; Navarro, C. Ring-Opening Polymerization of Trimethylene Carbonate Catalyzed by Methanesulfonic Acid: Activated Monomer versus Active Chain End Mechanisms. *Macromolecules* **2010,** *43* (21), 8828.
(51) Wang, X.; Thevenon, A.; Brosmer, J. L.; Yu, I.; Khan, S. I.; Mehrkhodavandi, P.; Diaconescu, P. L. Redox Control of Group 4 Metal Ring-Opening Polymerization Activity toward l-Lactide and ε-Caprolactone. *J. Am. Chem. Soc.* **2014,** *136* (32), 11264.
(52) Xu, X.; Luo, G.; Mehmood, A.; Zhao, Y.; Zhou, G.; Hou, Z.; Luo, Y. Theoretical Mechanistic Studies on Redox-Switchable Polymerization of Trimethylene Carbonate Catalyzed by an Indium Complex Bearing a Ferrocene-Based Ligand. *Organometallics* **2018,** *37* (24), 4599.
(53) Xu, X.; Luo, G.; Hou, Z.; Diaconescu, P. L.; Luo, Y. Theoretical insight into the redox-switchable activity of group 4 metal complexes for the ring-opening polymerization of ε-caprolactone. *Inorg. Chem. Front.* **2020,** *7* (4), 961.
(54) Pangborn, A. B.; Giardello, M. A.; Grubbs, R. H.; Rosen, R. K.; Timmers, F. J. Safe and Convenient Procedure for Solvent Purification. *Organometallics* **1996,** *15* (5), 1518.

(55) Dhar, D.; Yee, G. M.; Spaeth, A. D.; Boyce, D. W.; Zhang, H.; Dereli, B.; Cramer, C. J.; Tolman, W. B. Perturbing the Copper(III)–Hydroxide Unit through Ligand Structural Variation. *J. Am. Chem. Soc.* **2016,** *138* (1), 356.

TOC graphic

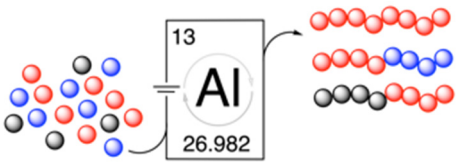

The electrochemically switchable reactivity of (salfen)Al(O^{i}Pr) (salfen = 1,1′-di(2,4-bis-*tert*-butyl-salicylimino)ferrocene) toward the ring opening polymerization of various cyclic esters, ethers, and carbonates was investigated.